Thermoelectric response in the incoherent transport region near Mott transition: The case study of La$_{1-x}$Sr$_x$VO$_3$

M. Uchida,[1] K. Oishi,[1] M. Matsuo,[2,3] W. Koshibae,[4] Y. Onose,[1,5] M. Mori,[2,3] J. Fujioka,[5] S. Miyasaka,[6]
S. Maekawa,[2,3] and Y. Tokura[1,4,5]

[1]*Department of Applied Physics, University of Tokyo, Tokyo 113-8656, Japan*
[2]*Advanced Science Research Center, Japan Atomic Energy Agency (JAEA), Tokai, Ibaraki 319-1195, Japan*
[3]*CREST, Japan Science and Technology Agency (JST), Tokyo 102-0075, Japan*
[4]*Cross-Correlated Materials Research Group (CMRG) and Correlated Electron Research Group (CERG), ASI, RIKEN,
Wako 351-0198, Japan*
[5]*Multiferroics Project, ERATO, Japan Science and Technology Agency (JST), Tokyo 113-8656, Japan*
[6]*Department of Physics, Osaka University, 1-1 Machikaneyama, Toyonaka, Osaka 560-0043, Japan*

We report a systematic investigation on the high-temperature thermoelectric response in a typical filling-control Mott transition system La$_{1-x}$Sr$_x$VO$_3$. In the vicinity of the Mott transition, incoherent charge transport appears with increasing temperature and the thermopower undergoes two essential crossovers, asymptotically approaching the limit values expected from the entropy consideration, known as the Heikes formula. By comparison with the results of the dynamical mean-field theory, we show that the thermopower in the Mott critical state mainly measures the entropy per charge carrier that depends on electronic degrees of freedom available at the measurement temperature. Our findings verify that the Heikes formula is indeed applicable to the real correlated electron systems at practical temperatures ($T > 200$ K).

I. INTRODUCTION

Thermoelectric materials, which interconvert temperature gradients and electric voltages, could play a key role for future energy production and utilization.[1] While the conventional research and optimization of the thermoelectric materials have been done based on the one-electron band theory, transition-metal oxides with strong electron correlation have recently attracted much attention as promising candidates since the discovery of unusually large thermopower S in Na$_x$CoO$_2$.[2,3] One possible origin of the enhanced S in the correlated metals is entropy flow of the correlated electrons,[4–8] expressed as the Heikes formula.[9,10] This mechanism could provide a strategy for designing the high-performance thermoelectric materials in a different way from the band-theory approach. However, the Heikes formula is strictly correct only in the high-temperature limit,[9,10] and its applicability at practical temperatures is highly nontrivial. It has been suggested by some groups that the large S observed in Na$_x$CoO$_2$ can be explained within some band-structure effects,[11–13] and the applicability of the Heikes formula to real materials is still under debate.

As derived by the Boltzmann transport equation in the band theory, conventional metals show the very small S well below the Fermi temperature $T_F \sim 10^4$ K, because it is strongly reduced by the factor T/T_F from the value $k_B/e \simeq 86$ μV/K. In the high-temperature limit, on the other hand, the conducting state is treated as the incoherent hopping of localized charge carriers between the adjacent sites and, hence, S derived by the Heikes formula becomes of the order of k_B/e, reflecting the entropy consideration. In materials with strong electron correlation, there exist two possible cases for the high-temperature regime ($k_B T \gg W$): (i) $k_B T \ll U$ or (ii) $U \ll k_B T$, where W is the half bandwidth and U is the on-site Coulomb interaction. In the case of $k_B T \ll U$,

S obtained from the Heikes formula is expressed as

$$S_1 = -\frac{k_B}{e} \ln \frac{g_e}{g_h} - \frac{k_B}{e} \ln \frac{x}{1-x}, \qquad (1)$$

where x is the hole concentration and g_e (g_h) denotes the local degeneracy of the electronic configuration on the site without (with) hole carrier.[4–6] In this temperature region, the spin and orbital degrees of freedom explicitly contribute to S. For $U \ll k_B T$, the carrier hopping occurs, allowing the doubly occupied states, and S is given by

$$S_2 = -\frac{k_B}{e} \ln \frac{2m-n}{n}, \qquad (2)$$

where m and n are the orbital degeneracy and the electron number per site, respectively.[9,10] Therefore, it is predicted that high-temperature S in the correlated metals shows crossovers asymptotically approaching the large limit values S_1 and S_2. In addition, depending on the signs of S_1 and S_2, the temperature dependence of S could be nonmonotonic as accompanied by nontrivial sign changes, while the sign of S in the conventional metals is determined by the sign of charge carrier. It is expected that, by observing such crossovers of S, the applicability of the Heikes formula can be experimentally verified.

As a model system suitable for examining the Heikes formula, we chose a canonical filling-control insulator-metal (Mott) transition system La$_{1-x}$Sr$_x$VO$_3$,[14–16] where a metallic state with coherent charge transport realizes only at low temperatures and the incoherent charge transport appears above ~200 K centered around the critical doping level x_{IM}. Thus, around x_{IM}, S is anticipated to asymptotically approach the Heikes-formula values with increasing temperature in a manner dependent on the doping level and the Coulomb correlation. By measuring S up to 1250 K and comparing to the results of dynamical mean-field theory (DMFT) for the

Hubbard model, we have clarified the essential features of the correlation effect on the high-temperature S and verified the applicability of the Heikes formula to the real correlated electron systems.

II. EXPERIMENTAL AND CALCULATION PROCEDURES

Single-crystalline ($x = 0$–0.26) and polycrystalline ($x = 0$–0.80) samples of $La_{1-x}Sr_xVO_3$ were prepared by a floating-zone method and solid-state reaction, respectively, as described elsewhere.[17] Polarized reflectivity spectra in the temperature range of 10–800 K were measured on the single crystals between 0.01 and 6 eV. The reflectivity spectra between 5 and 40 eV were measured at room temperature with use of synchrotron radiation at UV-SOR, Institute for Molecular Science. For the Kramers-Kronig analysis, the spectrum above 40 eV was extrapolated by the ω^{-4} function, while below 0.01 eV, the Hagen-Rubens relation or the constant reflectivity was assumed depending on the ground-state nature (metal or insulator). S was measured using a conventional steady-state technique in a cryostat (an electric furnace) below (above) room temperature. A temperature gradient was generated by heating (cooling) one edge of the sample with a small resistive heater (an air pump). The contribution of Au (Pt) wires for electrical contact was carefully subtracted. While x in the obtained single crystals is limited up to 0.26, S shows the nearly identical temperature and doping dependence between the single-crystalline and polycrystalline samples as shown later and, thus, we discuss the doping variation of S mainly based on the results of the polycrystals prepared in a wider doping region. All the measurements above room temperature were performed in a flow of Ar/H_2 (93%/7%) gas to prevent the oxidation, and we confirmed that the sample degradation at elevated temperature was negligible for the thermally repeated measurements.

For the DMFT calculation in the single-band Hubbard model, the iterated perturbation theory was used to solve the effective impurity problem. This solution is suitable for capturing general features of the correlation effects over a wide temperature. Semicircular density of states with the bandwidth of $2W$ was imposed on the noninteracting part of the Hamiltonian.

III. RESULTS AND DISCUSSION

Figure 1 shows the temperature dependence of the resistivity in $La_{1-x}Sr_xVO_3$ up to high temperature. The end compound $LaVO_3$ ($x = 0$), a prototypical Mott insulator with the V electron configuration of $3d^2$, undergoes the successive spin ordering (SO) and orbital ordering (OO) transitions at $T_{SO} = 143$ K (Ref.[18–20]) and $T_{OO} = 141$ K.[17,21] As shown in Fig. 1 the resistivity decreases dramatically with increasing the hole-doping level x,[22,23] and then shows the insulator-metal transition at $x_{IM} = 0.176$, accompanying the melting of the orbital order.[17,24] Above x_{IM}, the resistivity shows a metallic behavior; the difference observed between the single-crystalline and polycrystalline samples are due to grain boundary effects. Above 200 K, the resistivity in the single crystals asymptotically approaches the saturation values, indicating the incoherent charge transport.
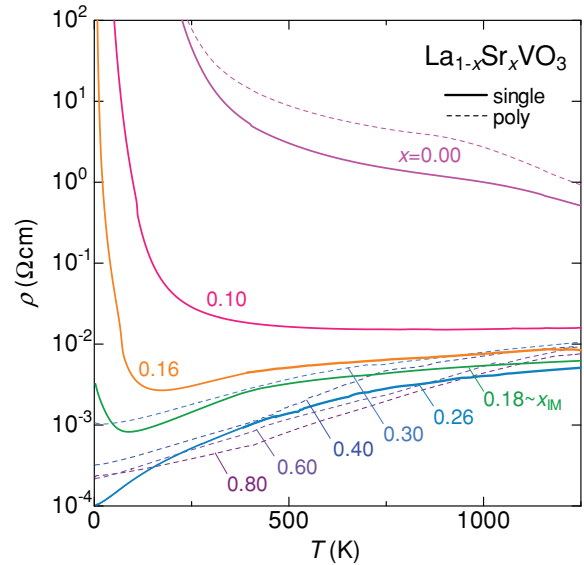

FIG. 1. (Color online). Temperature dependence of the resistivity ρ in $La_{1-x}Sr_xVO_3$. The solid and dashed lines represent the data for the single crystals and polycrystals, respectively.

In Fig. 2(a), we show the doping variation of the optical conductivity spectra at $T = 10$ K for the light polarization parallel to the c axis (E $\parallel$ c). With increasing x, the spectral weight of the Mott-gap excitation around 2 eV decreases, while the mid-infrared (mid-IR) peak appears in the inner-gap region and then evolves into the Drude peak at around x_{IM}.[24,25] As shown in Figs. 2(b) and 2(c), the low-energy ($\hbar\omega < 0.2$ eV)
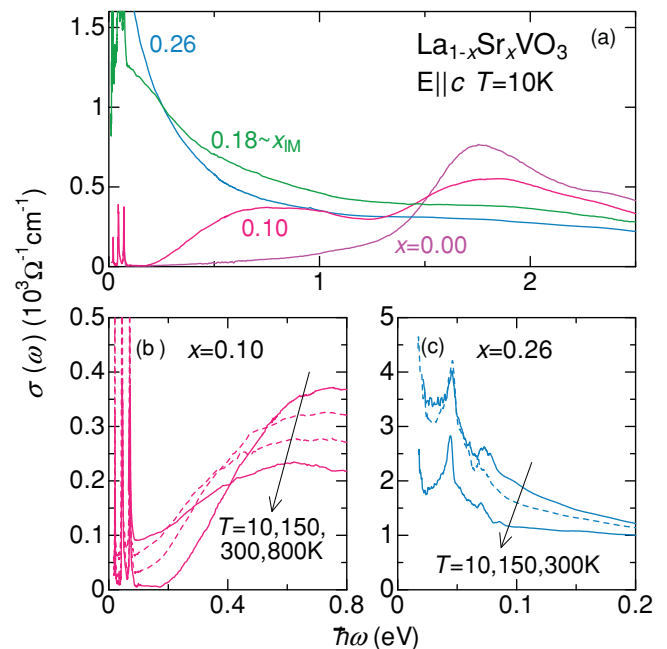

FIG. 2. (Color online). (a) Doping variation of the optical conductivity spectra at $T = 10$ K for the light polarization parallel to the c axis (E $\parallel$ c). Temperature dependence of the optical conductivity spectra for (b) $x = 0.10$ and (c) 0.26 up to high temperature. The ω-flat features appear with increasing temperature, indicating the incoherent charge dynamics.
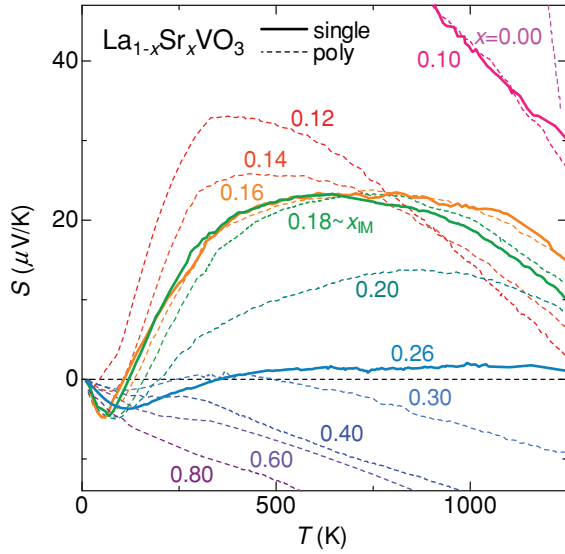
FIG. 3. (Color online). Temperature dependence of the thermopower S in $La_{1-x}Sr_xVO_3$. The solid and dashed lines represent the data for the single crystals and polycrystals, respectively.

optical conductivity spectra near x_{IM} tends to show a broadened feature with increasing temperature, indicating the incoherent charge dynamics; for $x = 0.10$, the mid-IR peak evolves into the ω-flat structure, accompanying the closing of the gap. Also, for $x = 0.26$, the sharp Drude peak changes to the rather ω-flat feature with increasing temperature.

In Fig. 3 we show the temperature variation of S in $La_{1-x}Sr_xVO_3$ up to 1250 K. Below $x \simeq 0.1$, S shows large positive values and decreases with increasing temperature, being typical of insulators or semiconductors. Above $x \simeq 0.4$, it shows linear T dependence with a small slope, which represents the conventional metallic feature. On the other hand, nonmonotonic temperature dependence is observed centered around x_{IM}; the enhanced negative slope at low temperatures around x_{IM} indicates the correlated metallic state with the enhanced carrier mass on the verge of the Mott transition,[26] which has also been confirmed by the measurement of the electronic specific-heat coefficient in this system.[17] With increasing temperature, S changes its sign at $T \sim 200$ K, and then reaches a relatively large positive value ($\gtrsim 20 \mu$V/K) at $T \sim 600$ K. As described above, the results of the resistivity and the optical conductivity indicate that the incoherent transport appears above 200 K around x_{IM}. Therefore, the change to the large positive values can be interpreted as the crossover to the high-temperature regime where the Heikes formula holds valid.

Figure 4(a) depicts the evolution of S as the contour map in the T-x plane. The regions below $x \simeq 0.1$ and above $x \simeq 0.4$ indicate the prototypical insulating and band-metallic state, respectively. In contrast, we can clearly see the region with large gradient of S above 200 K centered around x_{IM}, in which the incoherent charge dynamics is observed and the Heikes formula is expected to be applicable.

The observed variation of S around x_{IM} is explained in terms of the two crossovers approaching the high-temperature limit values obtained from the Heikes formulas of Eqs. (1) and (2), while S is negative at low temperatures reflecting the sign
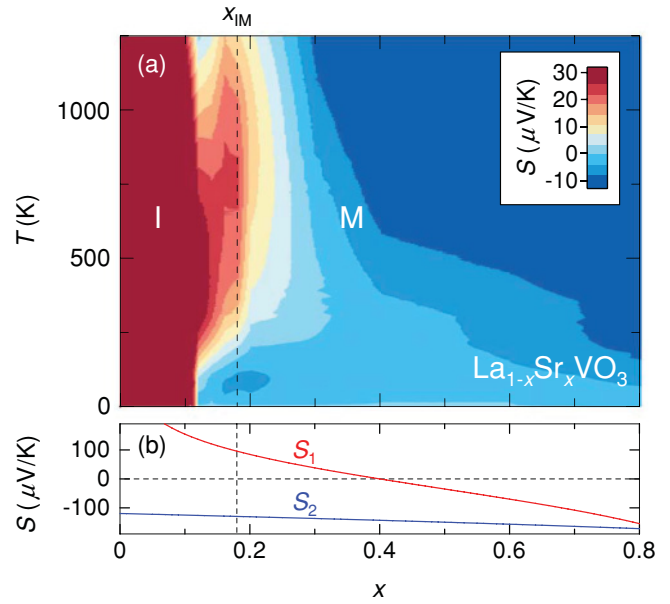

FIG. 4. (Color online). (a) Evolution of the thermopower S in the T-x phase diagram. The vertical dashed lines indicate the critical doping level x_{IM} for the insulator (I)-metal (M) transition at the ground state. The region with large S-gradient around x_{IM} corresponds to the incoherent metallic state as expected for the Heikes formula to be valid. (b) Doping variation of S in two high-temperature limits S_1 ($k_BT \ll U$) and S_2 ($U \ll k_BT$) in the Heikes formula with consideration of nearly degenerate t_{2g} or (t_{2g} plus e_g) orbitals (see text).

of the charge carrier. The theoretical asymptotic values in the high-temperature limits show the x dependence, as shown in Fig. 4(b), which is obtained by applying the Heikes formula to the $La_{1-x}Sr_xVO_3$ system. In the case of $k_BT \ll U$, the configurations are $g_e = 9$ and $g_h = 6$ for V^{3+} ($3d^2$) and V^{4+} ($3d^1$) ions, respectively, and Eq. (1) is expressed as

$$S_1 = -\frac{k_B}{e} \ln \frac{3x}{2(1-x)}. \quad (3)$$

Here, we assumed that the crystal field splitting (E_c) between the t_{2g} and e_g states and the Hund's-rule coupling energy (J_H) are all comparable to or smaller than U, but much larger than k_BT. For $U, E_c, J_H \ll k_BT$, on the other hand, inserting $m = 5$ and $n = 2 - x$ into Eq. (2), we have

$$S_2 = -\frac{k_B}{e} \ln \frac{8+x}{2-x}. \quad (4)$$

Around x_{IM}, the limit values S_1 and S_2 are positive and negative, respectively. Thus, the sign change at the characteristic temperature $T^* \sim 200$ K is due to the crossover asymptotically approaching S_1, where the charge transport changes from the coherent motion in the correlated metal to the carrier hopping as in a doped Mott insulator. Reflecting the doping variation of S_1, to which the spin and orbital degrees of freedom explicitly contribute, the maximum value of S in the intermediate temperature monotonically decreases with increasing x up to $x \simeq 0.3$, as shown in Fig. 3. With further increasing temperature, S begins to decrease while approaching negative S_2. This may correspond to another crossover to the incoherent metal state allowing the doubly occupied states. All these experimental results reveal that the
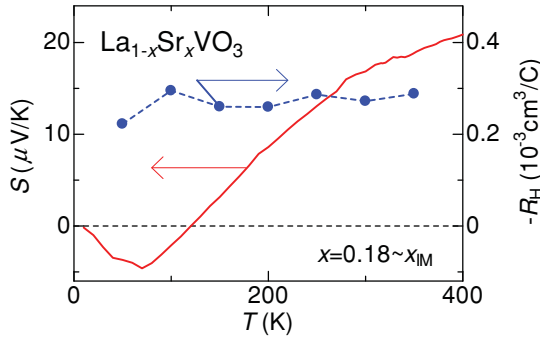
FIG. 5. (Color online). Comparison of temperature dependence between the thermopower S and the Hall coefficient R_H at $x = 0.18$.

FIG. 6. (Color online). (a) Selected experimental data of the temperature and doping variation of the thermopower S in $La_{1-x}Sr_xVO_3$ for comparison with the theoretical results (b) and (c). Variation of S with (b) doping x and (c) Coulomb interaction U obtained by the DMFT calculations on the single-band Hubbard model.

energy scales $k_B T$ (~ 20 and 120 meV) as corresponding to two crossover temperatures appear still smaller than the anticipated W and U values. This should be considered not as a discrepancy from the assumption in the derivation of S_1 and S_2 [Eqs. (3) and (4)], but as a reflection of the high sensitivity of S to the entropy transport. Such an *undershooting* behavior of the S crossovers is also partly reproduced in the simple DMFT calculation (*vide infra*).

Figure 5 shows the temperature dependence of the Hall coefficient R_H at $x = 0.18$ ($\sim x_{IM}$), as a typical example. R_H still shows nearly constant negative values reflecting the sign of the charge carrier, while S changes its sign from negative to positive. The contrasting behavior between S and R_H comes from the high sensitivity of S to the entropy transport, and indeed ensures that the S crossovers can not be explained by the change of the band structure around the Fermi level. Thus, comparison with a model calculation, which may be simple but fully takes into account the correlation effects, will be useful to capture the essence of the high temperature S.

The remarkable variation of S in the Mott critical state, as typified by the sign changes of S centered around x_{IM}, is shown using the selected experimental data set of Fig. 6(a). Figures 6(b) and 6(c) show results of the DMFT calculation of S with the doping rate x and the ratio of U/W, respectively. In this calculation, the energy gradient of density of states at Fermi level is positive at $k_B T = 0$ and, thus, S at low temperatures is negative since $-S$ is approximately proportional to the gradient. In the high-temperature limit, on the other hand, S must asymptotically approach the limit values given by

$$S_1 = -\frac{k_B}{e} \ln \frac{2x}{1-x} \qquad (5)$$

for the case $k_B T \ll U$ ($g_e = 2$, $g_h = 1$) and

$$S_2 = -\frac{k_B}{e} \ln \frac{1+x}{1-x} \qquad (6)$$

for the case $U \ll k_B T$ ($m = 1$, $n = 1 - x$). For $x = 0.2$, as an example, the limit values S_1 and S_2 are positive and negative, respectively, and thus S should change its sign twice in the whole temperature region, as in the case of $La_{1-x}Sr_xVO_3$. As shown in Fig. 6(b), S at $x = 0.2$ indeed shows the nonmonotonic temperature dependence analogous to the experimentally observed one. With increasing x, S_1 decreases and finally changes the sign, while the absolute value $|S_2|$ increases monotonically. Besides, the Coulomb
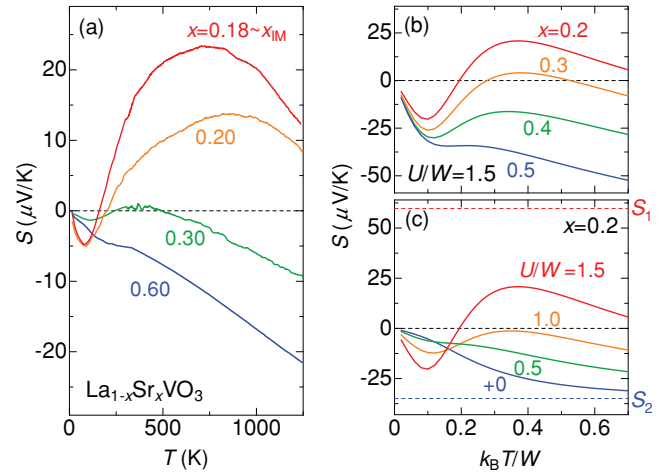
interaction becomes less effective for larger x or in going away from the half filling; this explains the detailed x dependence of the asymptotic behavior of S [Fig. 6(b)]. Of course, except in the strong-correlation ($U \gg W$) and high-temperature ($k_B T \gg W$) limits, S is not in agreement with the limit values S_1 and S_2. As shown in Fig. 6(c), in the case of $U/W = 1.5$, S indeed shows the approach to S_2 before fully approaching S_1 ($\sim 60\,\mu V/K$). With decreasing U, S tends to directly approach S_2 ($\sim -35\,\mu V/K$), while the carrier mass enhancement, manifesting as a steep negative T-gradient at low temperatures, disappears. These theoretical results can reproduce the experimentally observed features for $La_{1-x}Sr_xVO_3$, confirming that the effect of Coulomb interaction is essential for the observed nonmonotonic temperature dependence of S.

IV. CONCLUSION

Our systematic investigations on $La_{1-x}Sr_xVO_3$ thus show that, in the incoherent transport region above $T^* \sim 200$ K, S measures the entropy per charge carrier in response to the magnitude relation between $k_B T$, W, and U (and E_c, J_H), and thus shows the two essential crossovers, asymptotically approaching, respectively, the limit values S_1 and S_2 obtained from the Heikes formulas. In the case of some metallic-layered cobaltites including Na_xCoO_2, typical thermoelectric materials with the strong electron correlation, the limit values have the same positive sign as the low-temperature one determined by the band structure, and thus it would be difficult to detect the S crossovers. Recently, however, a similar crossover at T^* (~ 200 K) has been suggested for Na_xCoO_2 by temperature-dependent photoemission spectroscopy;[27] the unchanged sign of S may be one of the origins of the large S observed in these compounds.[28] The present findings unravel the generic features of the correlation effects on the high-temperature thermoelectric response and demonstrate the possibility that the Heikes formula can be indeed useful for the design of the correlated thermoelectric materials at practical temperatures ($T > 200$ K), not necessarily in the high-temperature limit.

[1] G. Mahan, B. Sales, and J. Sharp, Phys. Today **50**, 42 (1997).

[2] I. Terasaki, Y. Sasago, and K. Uchinokura, Phys. Rev. B **56**, 12685(R) (1997).

[3] M. Lee, L. Viciu, L. Li, Y. Wang, M. L. Foo, S. Watauchi, R. A. Pascal Jr., R. J. Cava, and N. P. Ong, Nat. Mater. **5**, 537 (2006).

[4] W. Koshibae, K. Tsutsui, and S. Maekawa, Phys. Rev. B **62**, 6869 (2000).

[5] W. Koshibae and S. Maekawa, Phys. Rev. Lett. **87**, 236603 (2001).

[6] S. Maekawa, T. Tohyama, S. E. Barnes, S. Ishihara, W. Koshibae, and G. Khaliullin, *Physics of Transition Metal Oxides* (Springer, Berlin, 2004).

[7] Y. Wang, N. S. Rogado, R. J. Cava, and N. P. Ong, Nature (London) **423**, 425 (2003).

[8] G. Pálsson and G. Kotliar, Phys. Rev. Lett. **80**, 4775 (1998).

[9] R. R. Heikes and R. W. Ure, *Thermoelectricity: Science and Engineering* (Interscience, New York, 1961).

[10] P. M. Chaikin and G. Beni, Phys. Rev. B **13**, 647 (1976).

[11] D. J. Singh, Phys. Rev. B **61**, 13397 (2000).

[12] T. Takeuchi, T. Kondo, T. Takami, H. Takahashi, H. Ikuta, U. Mizutani, K. Soda, R. Funahashi, M. Shikano, M. Mikami, S. Tsuda, T. Yokoya, S. Shin, and T. Muro, Phys. Rev. B **69**, 125410 (2004).

[13] K. Kuroki and R. Arita, J. Phys. Soc. Jpn. **76**, 083707 (2007).

[14] N. F. Mott, *Metal Insulator Transitions* (Taylor and Francis, London, 1990).

[15] M. Imada, A. Fujimori, and Y. Tokura, Rev. Mod. Phys. **70**, 1039 (1998).

[16] F. Inaba, T. Arima, T. Ishikawa, T. Katsufuji, and Y. Tokura, Phys. Rev. B **52**, R2221 (1995).

[17] S. Miyasaka, T. Okuda, and Y. Tokura, Phys. Rev. Lett. **85**, 5388 (2000).

[18] V. G. Zubkov, G. V. Bazuev, V. A. Perelyaev, and G. P. Shveiken, Fiz. Tverd. Tela (Leningrad) **15**, 1610 (1973) [Sov. Phys. Solid State **15**, 1079 (1973)].

[19] A. V. Mahajan, D. C. Johnston, D. R. Torgeson, and F. Borsa, Phys. Rev. B **46**, 10966 (1992).

[20] P. Bordet, C. Chaillout, M. Marezio, Q. Huang, A. Santoro, S. W. Cheong, H. Takagi, C. S. Oglesby, and B. Batlogg, J. Solid State Chem. **106**, 253 (1993).

[21] S. Miyasaka, Y. Okimoto, M. Iwama, and Y. Tokura, Phys. Rev. B **68**, 100406(R) (2003).

[22] P. Dougier and P. Hagenmuller, J. Solid State Chem. **15**, 158 (1975).

[23] A. V. Mahajan, D. C. Johnston, D. R. Torgeson, and F. Borsa, Phys. Rev. B **46**, 10973 (1992).

[24] J. Fujioka, S. Miyasaka, and Y. Tokura, Phys. Rev. Lett. **97**, 196401 (2006).

[25] S. Miyasaka, Y. Okimoto, and Y. Tokura, J. Phys. Soc. Jpn. **71**, 2086 (2002).

[26] W. F. Brinkman and T. M. Rice, Phys. Rev. B **2**, 4302 (1970).

[27] Y. Ishida, H. Ohta, A. Fujimori, and H. Hosono, J. Phys. Soc. Jpn. **76**, 103709 (2007).

[28] K. Haule and G. Kotliar, *Properties and Applications of Thermoelectric Materials*, edited by V. Zlatić and A. C. Hewson (Springer, New York, 2009).